The behaviour of mineral matter during combustion of Spanish subbituminous and brown coals

X. Querol, J. L. Fernandez Turiel and A. Lopez Soler

Institute of Earth Sciences "Jaime Almera", CSIC, C/Marti i Franques s/n 08028, Barcelona, Spain

Abstract

Combustion experiments up to 1400°C were carried out with subbituminous coals from the Teruel power station, the Teruel Mining District, the Santa Eulalia coal deposit and with lignite from the As Pontes power station in Spain. The characterisations of the occurrence and distribution of inorganic matter and its transformation during combustion of these coals were carried out by means of X-ray diffraction and optical and electron microscopy. The combustion experiments show that the inorganic transformations during the combustion of all the coals studied vary depending on the sulphur and calcium contents. The sulphur, iron and calcium contents govern the quality of anhydrite crystallisation (which takes place between 600 and 900°C. Furthermore, the high calcium oxide content produces the fouling of the combustion wastes at relatively low temperatures (1200°C), prevents the occurrence of mullite and magnetite in the ashes and leads to the crystallisation of anorthite and esseneite during the cooling. The comparison of the inorganic phases of fly ashes and slags from the Teruel power station with those of the experimental wastes shows that the inorganic transformations during coal combustion in the power station can be predicted by means of laboratory furnace experiments provided that the residence time in the flame and the effect of the cooling and evacuation controls of gases and particles from the power station are taken in consideration.

KEYWORDS: coal, coal combustion, mineral matter, X-ray diffraction.

Introduction

THE growing interest in the study of mineral matter in coals is due to its important role in the physico-chemical transformations during coal combustion (Raask, 1985). All these transformation processes exert an influence over the environmental quality of the areas surrounding the power generation plants.

The mineral matter content and composition are important parameters in coal quality characterization and, consequently, in coal use designation. Mineralogical studies should be carried out to characterise the inorganic fraction of coals since the chemical analyses give only partial information required for the prediction of the behaviour of some elements during the coal conversion processes. Thus, the importance of mineralogical studies on the occurrence and distribution of S, Ca and Na-bearing phases in coal must be emphasised (Finkelman, 1982). Studies on the behaviour of S-bearing minerals during coal cleaning and combustion may help to minimize the sulphur emissions resulting from coal combustion processes, whereas experimental studies on the Ca-Na-bearing phase transformations during coal combustion may help to predict fouling problems.

During coal combustion in power stations a series of physico-chemical transformations results in transference of potentially toxic elements to the surrounding environment (Raask, 1985; Smith, 1987) through combustion gases and the finest fly ashes that escape from the particulate controls. The pathways and the amounts of the potentially

toxic element emission depend on fuel quality and on combustion technology (Smith, 1987).

Although sintering, fusion, fouling and slagging processes in coal ashes are currently well known, there is need for research on the inorganic transformations during the coal combustion. Several studies have been carried out on the mineral matter occurrence in Spanish brown coals (Felgueroso *et al.*, 1988; Martinez-Alonso *et al.*, 1987; Martinez-Tarazona *et al.*, 1990; Querol, 1990; Querol *et al.*, 1989, 1990). The present work focuses on the occurrence and the distribution of inorganic matter in Spanish subbituminous coals and lignites and in its transformations during combustion, with special reference to the coal from the Teruel power station (1050 MW) in NE Spain.

Experimental

A representative coal sample of 140 kg from the Teruel power station (15000 t coal/day) was studied. Twenty kilograms of coal per day were sampled for seven days after splitting 2000 t coal with an automatic sampler. The whole sample was air dried, milled and split following the ISO recommendations to obtain a coal sample of 1 kg milled under 0.25 mm. For a detailed mineralogical study, eleven density fractions between < 1.3 and > 2.8 g/cc were obtained from the whole coal sample by using bromoform, tetrachlorethylene and xylene.

In order to study the inorganic transformations during coal combustion, combustion experiments

were carried out with the Teruel coal using a laboratory furnace. Samples were obtained at 110, 250, 350, 400, 450, 550, 600, 750, 850, 950, 1100, 1200 and 1400°C. The same combustion experiments were carried out with other Spanish subbituminous coals and lignites (Fig. 1) with the aim of comparing the behaviour of inorganic matter during the combustion of different coals. The selected coals samples were as follows:
(a) A representative coal sample from the 4th coal seam of the Sabrine Mine (Utrillas, Teruel, Fig. 1). Previous works (Querol 1990; Querol *et al.*, 1991) have shown that this coal seam has a medium quality level in the Albian (Cretaceous) coal deposits from the Teruel Mining District regarding mineral matter and sulphur contents and calorific power.
(b) A representative sample from the As Pontes power station (1450 MW), La Coruña (Fig. 1). This Tertiary lignite is supplied to the power station from the As Pontes Mining District. The lignites show an organic affinity for some major elements such as Ca. These organically derived elements can have an important role in the physico-chemical reactions during the combustion.
(c) A representative sample from the Tertiary subbituminous coal from the Santa Eulalia Deposit in Teruel, Fig. 1. This coal deposit will be mined for power generation consumption in the near future.
(d) A mixture of the Santa Eulalia coal and limestone (1:10), to show the effect of calcium addition in the inorganic transformations during coal combustion.Finally, with the aim of comparing the inorganic phases of the experimental combustion wastes with those obtained from the combustion of the same coal in real conditions, the slags (in the ashers) and the fly ashes (in the electrostatic precipitators) were sampled for the same period of the coal sampling at the Teruel power station. For a detailed study, six density fractions between < 1.0 and > 2.8 g/cc were obtained from the whole fly ash sample by using bromoform, tetrachlorethylene and xylene.

All the samples obtained from the sampling, density deparations and the combustion experiments were mineralogically characterized by means of qualitative X-ray diffraction (XRD) and electron microscopy. The Reference Intensity Method (Chung, 1974 *a, b* 1975) using fluorite as the reference standard, was the method used for the XRD quantitative analysis. The XRD quantitative method used in this study is described in Querol *et al.* (1993). The Reference Intensity Method is based on the following equation:

FIG. 1. Location of the Spanish subbituminous coals and lignites studied in the present work. As Pontes power station (1450 MW), Teruel power station (1050 MW), Sabrina Mine in Utrillas (Province of Teruel), and Santa Eulalia coal deposit (Province of Teruel).

$$(I_i/I_f) = (X_i/X_f) K_i$$
$$X_i = (I_i/I_f) (X_f/K_i)$$
$$X_i + X_f + \ldots\ldots X_n = 100$$

where X_i and X_f are the concentrations of a mineral phase 'i' and the reference standard (fluorite in this work) in the sample, I_i and I_f their respective X-ray diffraction intensities, and K_i the intensity ratio between both the mineral phases 'i' and the reference standard in a binary mixture 1:1.

The mean relative errors obtained using the RIM for mineralogical quantitive analyses range from ± 4.60 (hematite) to ± 7.76 (anhydrite). The XRD patterns were obtained by using a powder diffractometer SIEMENS D500 with a graphite monochromator and NaI(Tl) detector and Cu $K\alpha$ radiation.

Mineral matter in the coals

The major mineral phases found are (Fig. 2): kaolinite, illite, gypsum, pyrite, marcasite, quartz, microcline and calcite. Furthermore, the following minor minerals were identified in coals from the Teruel Mining District: interlayered clays illite–smectite and iron sulphates with different hydration degrees (szomolnikite ($FeSO_4\cdot2H_2O$), rozenite ($FeSO_4\cdot4H_2O$), melanterite ($FeSO_4\cdot7H_2O$), jarosite (($Na,F)Fe_3(SO_4)_2(OH)_6$), etc). The density
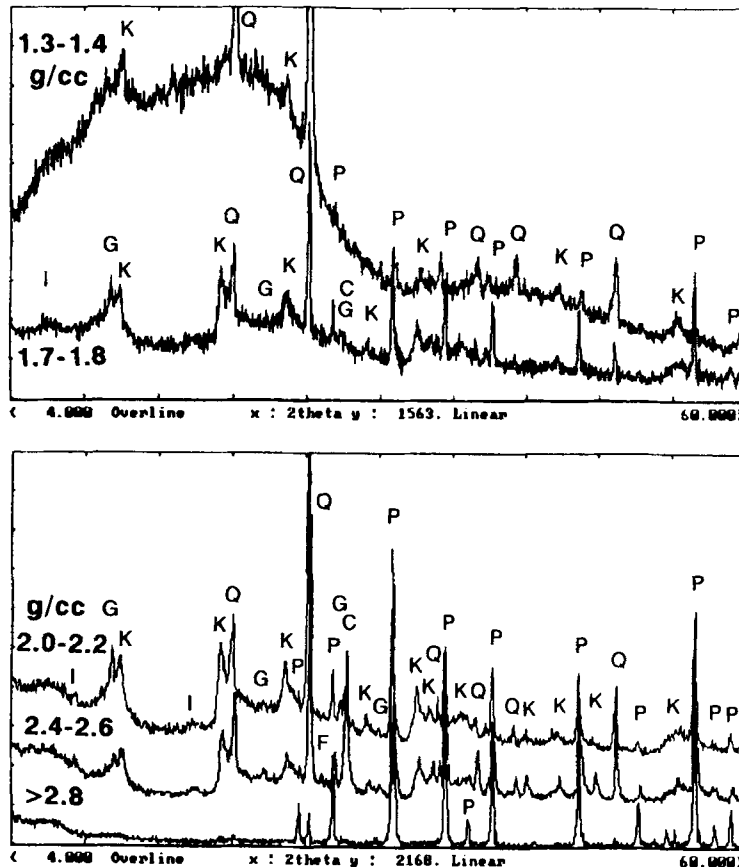

FIG. 2. X-ray diffraction patterns of the 1.3–1.4, 1.7–1.8, 2.0–2.2, 2.4–2.6 and > 2.8 g/cc density fractions from the Teruel power station coal. Note the presence of pyrite, clay minerals and quartz in the lighter fractions. C, calcite; F, feldspars; G, gypsum; I, illite; K, kaolinite; P, pyrite and/or marcasite; and Q, quartz. Note the high XRD background in the light density fraction due to the high organic matter content.
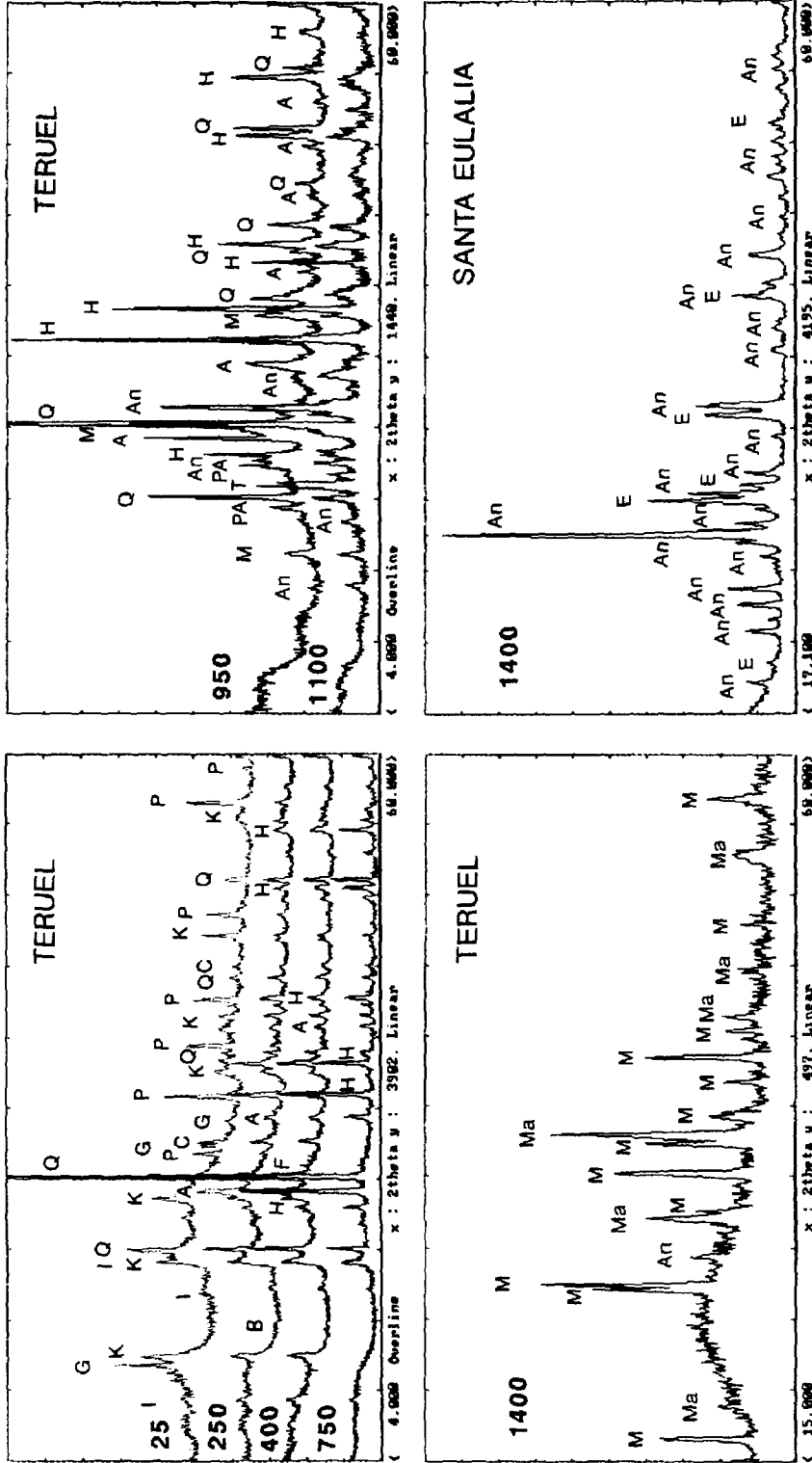
FIG. 3. X-ray diffraction patterns of the combustion wastes obtained at 25, 250, 400, 750, 950, 1100 and 1400°C from the combustion experiments of the Teruel power station coal and the Santa Eulalia coal with limestone addition at 1400°C. Note the differences in the inorganic phases of the ashes at 1400°C due to the calcium addition in the Santa Eulalia coal. A, anhydrite; An, anorthite; B, bassanite; C, calcite; E, esseneite; F, feldspars; G, gypsum; H, hematite; I, illite; K, kaolinite; M, mullite; Ma, magnetite; P, pyrite and/or marcasite; PA, pre-anorthite; Q, Quartz and T, tridymite.

TABLE 1. Yield values, high temperature ash (HTA, 750°C), mineral and organic matter contents and moisture of the different density fractions between 1.3 and 2.8 g/cc obtained from the Teruel coal. Results of X-ray diffraction quantification in % on air dried basis. *. Quantified by difference. Q, quartz; CL, clay minerals; K-F, K-feldspars; C, calcite; P-M, pyrite and marcasite; G, gypsum; OM, organic matter

Density (g/cc)	Yields	HTA	CL	Q	K-F	C	P-M	G	OM*	HR
1.3–1.4	8.1	7.2	4.6	2.9	<0.1	<0.1	0.2	<0.1	87.9	4.4
1.4-1.5	33.4	10.3	7.3	2.7	<0.1	<0.1	1.1	<0.1	78.8	10.1
1.5-1.6	20.2	20.2	16.4	3.6	<0.1	0.2	3.0	<0.1	67.9	8.9
1.6-1.7	10.5	27.5	24.6	3.4	<0.1	0.2	3.9	0.9	60.1	6.4
1.7-1.8	8.7	34.9	32.5	3.7	<0.1	0.3	4.7	1.2	48.2	9.4
1.8-2.0	8.3	44.3	41.3	4.1	<0.1	0.2	5.7	1.4	38.2	9.1
2.0-2.2	5.0	52.7	49.9	5.3	<0.1	2.1	7.0	1.7	25.5	8.5
2.2-2.4	2.1	64.2	56.2	7.0	<0.1	2.6	9.2	2.0	18.4	4.6
2.4-2.6	1.9	75.6	60.0	9.9	0.4	3.8	10.6	0.8	11.6	2.9
2.6-2.8	0.7	76.1	46.8	13.7	2.1	8.3	12.7	0.7	12.8	2.9
2.8	1.1	60.3	10.8	1.9	<0.1	0.1	73.6	<0.1	12.2	1.4

yields, high temperature ash contents (HTA, 750°C), organic matter (by difference) and mineral contents of the different density fractions between 1.3 and 2.8 g/cc, are given in Table 1.
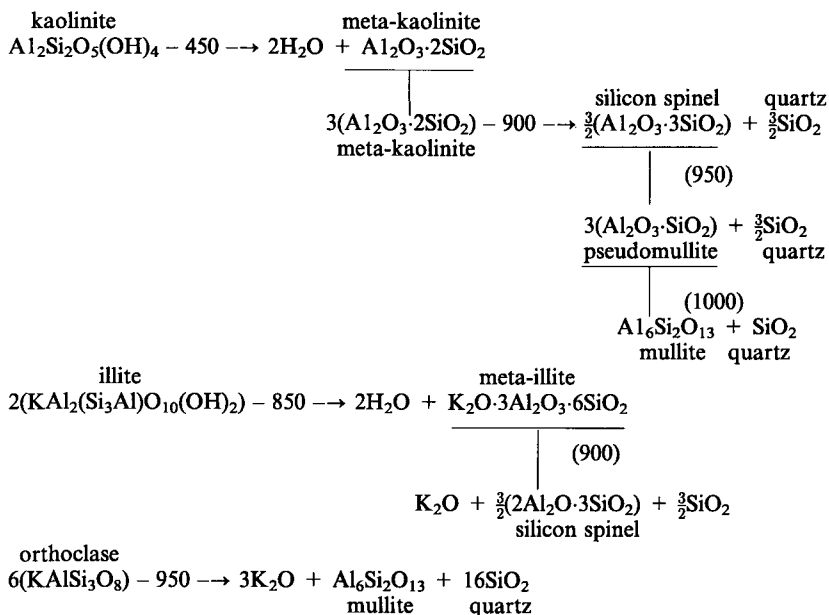
The density fraction yields show that the fractions 1.4–1.6 g/cc and 1.4–2.2 g/cc represent more than 50% and 85% of the whole coal weight, respectively. The HTA content increases with density increase, but there is a decrease in the HTA content in the >2.8 g/cc coal fraction since in this fraction the mineral matter predominantly comprises iron sulphides, and these minerals experience thermal decomposition (with SO_2 volatilization) at the ashing temperature.
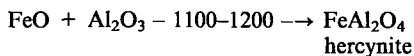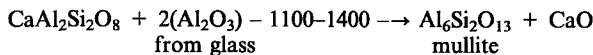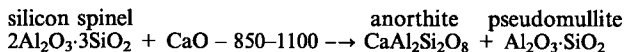
TABLE 2. Inorganic phases content of the experimental combustion wastes of the Teruel coal. Results of X-ray diffraction quantification in % on air dried basis. *. Quantified by difference. T, temperature; R, residue; Q, quartz; Cl, clay minerals and/or amorphous aluminosilicate; K-F, K-feldspars; C, calcite; P-M, pyrite and marcasite; G, gypsum; B, bassanite; A, anhydrite; P-A, pre-anorthite; An, anorthite; M, mullite; H, hematite; Ma, magnetite; T, tridymite and OM-W, organic matter and organic matter plus water in the sample 25.

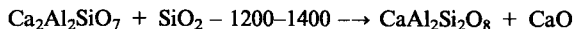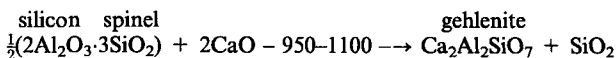| T(°C)	R	Q	Cl	K-F	C	P-M	G	B	A	P-A	An	M	H	Ma	T	OM*-W
25	100.0	3.9	25.5	<l.d.	0.4	4.4	1.5	0.0	0.0	0.0	0.0	0.0	0.0	0.0	0.0	64.3
110	93.4	4.0	25.6	<l.d.	0.4	4.6	0.0	1.2	0.0	0.0	0.0	0.0	0.0	0.0	0.0	57.5
250	56.8	3.8	25.6	<l.d.	0.3	2.8	0.0	0.0	1.2	0.0	0.0	0.0	1.4	0.0	0.0	21.7
350	46.5	3.7	25.5	0.4	0.2	1.2	0.0	0.0	1.2	0.0	0.0	0.0	1.4	0.0	0.0	13.1
400	39.0	4.1	20.5	0.4	0.2	0.6	0.0	0.0	1.1	0.0	0.0	0.0	1.4	0.0	0.0	10.7
450	28.5	3.9	19.0	0.4	0.2	0.0	0.0	0.0	1.5	0.0	0.0	0.0	1.6	0.0	0.0	1.9
500	28.5	3.8	19.0	0.3	0.2	0.0	0.0	0.0	1.9	0.0	0.0	0.0	1.7	0.0	0.0	1.6
550	28.4	4.0	19.0	0.2	0.1	0.0	0.0	0.0	2.1	0.0	0.0	0.0	1.7	0.0	0.0	1.3
600	28.1	4.0	18.9	0.2	0.1	0.0	0.0	0.0	2.2	0.0	0.0	0.0	2.7	0.0	0.0	0.0
750	27.2	3.8	17.4	0.2	0.05	0.0	0.0	0.0	2.8	0.0	0.0	0.0	2.9	0.0	0.0	0.0
850	26.5	3.7	17.4	0.0	0.0	0.0	0.0	0.0	1.9	0.5	0.3	0.0	2.7	0.0	0.0	0.0
950	25.6	3.7	15.8	0.0	0.0	0.0	0.0	0.0	1.0	0.7	0.5	1.0	2.4	0.0	0.5	0.0
1100	25.5	1.2	14.7	0.0	0.0	0.0	0.0	0.0	0.0	0.0	2.4	2.4	0.8	0.0	4.0	0.0
1200	25.5	0.2	20.3	0.0	0.0	0.0	0.0	0.0	0.0	0.0	0.3	3.6	1.1	0.0	0.0	0.0
1400	23.9	0.0	16.2	0.0	0.0	0.0	0.0	0.0	0.0	0.0	0.5	3.9	0.0	3.3	0.0	0.0

TABLE 3. Major mineral transformations of the aluminosilcate phases during the combustion of the Spanish brown coals depending on the calcium and iron contents. Temperature in degrees Celsius.
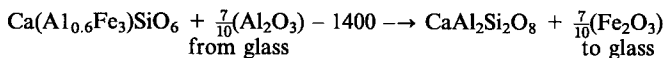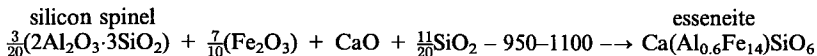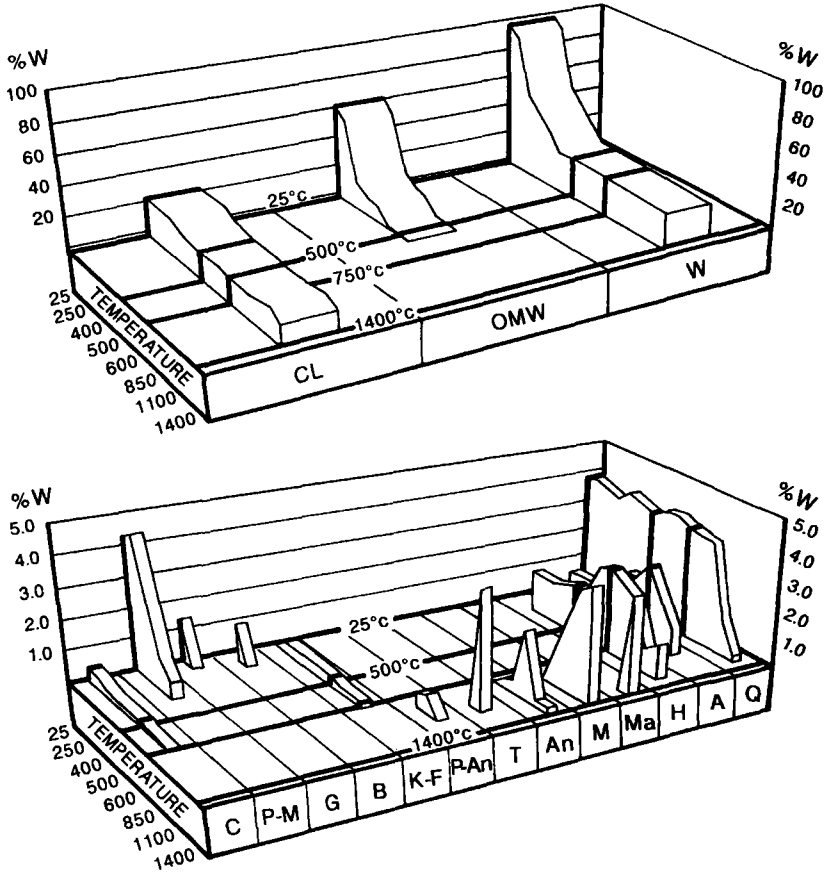
kaolinite   meta-kaolinite
$Al_2Si_2O_5(OH)_4 - 450 \longrightarrow 2H_2O + Al_2O_3 \cdot 2SiO_2$

$$\text{silicon spinel} \quad \text{quartz}$$
$$3(Al_2O_3 \cdot 2SiO_2) - 900 \longrightarrow \tfrac{3}{2}(Al_2O_3 \cdot 3SiO_2) + \tfrac{3}{2}SiO_2$$
meta-kaolinite

(950)

$$3(Al_2O_3 \cdot SiO_2) + \tfrac{3}{2}SiO_2$$
pseudomullite   quartz

(1000)
$$Al_6Si_2O_{13} + SiO_2$$
mullite   quartz

illite   meta-illite
$2(KAl_2(Si_3Al)O_{10}(OH)_2) - 850 \longrightarrow 2H_2O + K_2O \cdot 3Al_2O_3 \cdot 6SiO_2$

(900)

$$K_2O + \tfrac{3}{2}(2Al_2O \cdot 3SiO_2) + \tfrac{3}{2}SiO_2$$
silicon spinel

orthoclase
$6(KAlSi_3O_8) - 950 \longrightarrow 3K_2O + Al_6Si_2O_{13} + 16SiO_2$
mullite   quartz

If $[CaO] \uparrow$ and $[Fe_2O_3] \uparrow$ then,

silicon spinel   anorthite   pseudomullite
$2Al_2O_3 \cdot 3SiO_2 + CaO - 850{-}1100 \longrightarrow CaAl_2Si_2O_8 + Al_2O_3 \cdot SiO_2$

$CaAl_2Si_2O_8 + 2(Al_2O_3) - 1100{-}1400 \longrightarrow Al_6Si_2O_{13} + CaO$
       from glass   mullite

$FeO + Al_2O_3 - 1100{-}1200 \longrightarrow FeAl_2O_4$
hercynite

If $[CaO] \uparrow\uparrow\uparrow$ then,

silicon   spinel   gehlenite
$\tfrac{1}{2}(2Al_2O_3 \cdot 3SiO_2) + 2CaO - 950{-}1100 \longrightarrow Ca_2Al_2SiO_7 + SiO_2$

$Ca_2Al_2SiO_7 + SiO_2 - 1200{-}1400 \longrightarrow CaAl_2Si_2O_8 + CaO$

If $[CaO] \uparrow\uparrow\uparrow$ and $[Fe_2O_3] \uparrow$ then,

silicon spinel   esseneite
$\tfrac{3}{20}(2Al_2O_3 \cdot 3SiO_2) + \tfrac{7}{10}(Fe_2O_3) + CaO + \tfrac{11}{20}SiO_2 - 950{-}1100 \longrightarrow Ca(Al_{0.6}Fe_{14})SiO_6$

$Ca(Al_{0.6}Fe_3)SiO_6 + \tfrac{7}{10}(Al_2O_3) - 1400 \longrightarrow CaAl_2Si_2O_8 + \tfrac{7}{10}(Fe_2O_3)$
     from glass   to glass

TERUEL COAL

COAL COMBUSTION

FIG. 4. Weight evolution of the clay minerals and derived amorphous aluminosilicate (CL), organic matter (OMW), whole coal sample (W) and different inorganic phases during the combustion experiment of the Teruel power station coal. C, calcite; P-M, pyrite and marcasite; G, gypsum; B, bassanite; A, anhydrite; K-F, K-feldspars; P-An, pre-anorthite; T, tridymite; An, anorthite; M, mullite; H, hematite; Ma, magnetite; Q, quartz.

The iron sulphides (pyrite and marcasite) are present in the light density fractions with a fine grain size (between 1 and 20 μm) and dispersed in the organic matter. The sulphide content rises with the density increase, showing the highest sulphide content in the > 2.8 g/cc fraction, which is normal, bearing in mind that these sulphides have a density of 5.0 g/cc.

The quartz, feldspars and calcite (of 2.65, 2.63 and 2.94 g/cc density) show the highest concentration between the 2.4–2.8 g/cc fractions, the clay minerals between 2.2–2.6 g/cc, the gypsum between 1.8 and 2.4 g/cc, and the organic matter between 1.3 and 1.5 g/cc fractions (see Table 1).

These results show that the clay minerals, quartz and sulphides have a proportion of their content (with fine grain size) that is dispersed in the organic matter since these mineral phases are present in the light coal fractions (see Fig. 2), whereas the calcite, feldspars and gypsum are independent of the organic matrix.

Behaviour of mineral matter during coal combustion

The inorganic phases arising from the physico-chemical transformations of the coal inorganic matter during coal combustion are (Fig. 3):
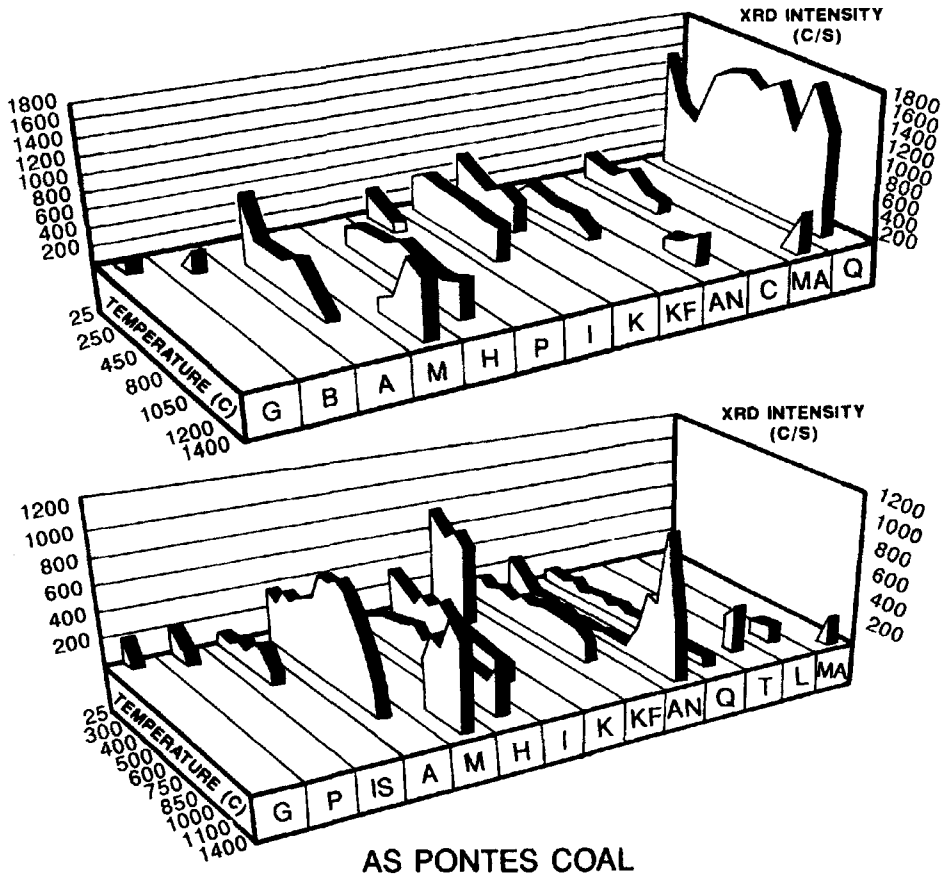
4th COAL SEAM, SABRINE MINE
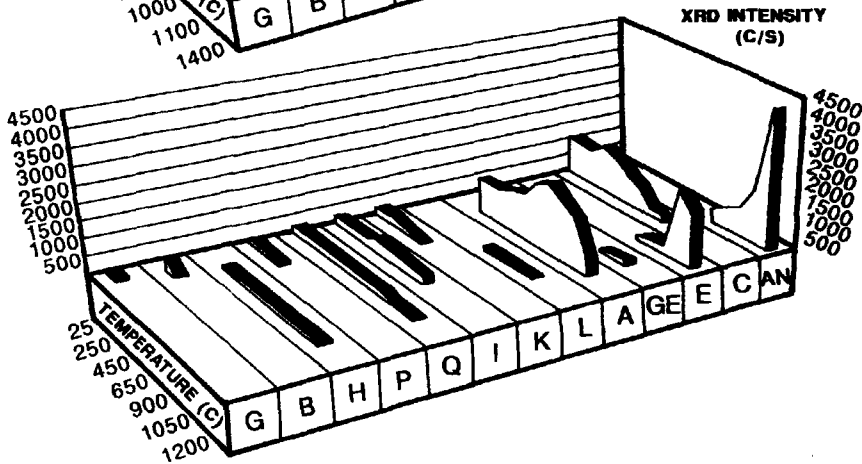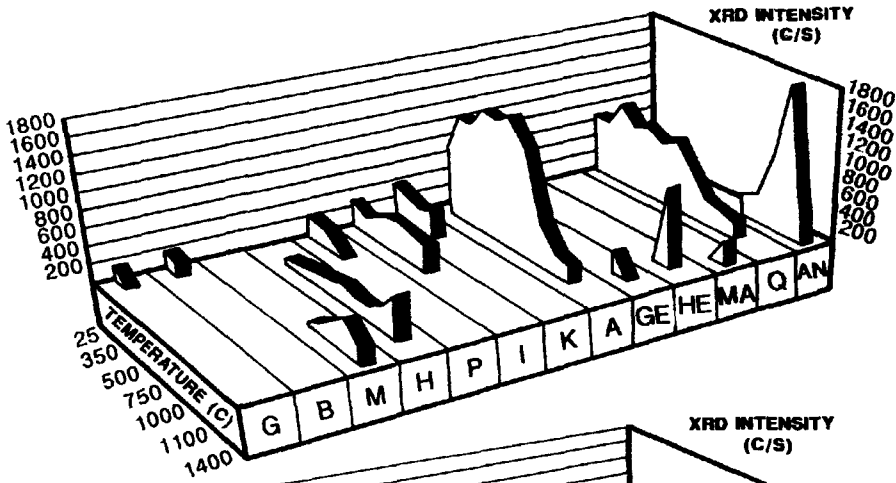

AS PONTES COAL

FIG. 5. Evolution of the different inorganic phases during combustion experiments on Sabrine Mine and As Pontes power station coals. C, calcite; P, pyrite; G, gypsum; B, bassanite; A, anhydrite; IS, iron sulphates; I, illite; K, kaolinite; K-F-, K-feldspars; T, tridymite; An, anorthite; M, mullite; L, lime; H, hematite; Ma, magnetite; Q, quartz. The absolute values for each phase are the intensity in counts per second (proportional to its concentration) of the maximum intensity peak of each phase in the X-ray diffraction pattern of the combustion wastes at different temperatures.

basanite, anhydrite, hematite, magnetite, calcium aluminosilicate which is a polymorph of anorthite, anorthite–albite, tridymite and mullite. The results obtained from the XRD quantification of these phases are shown in Table 2. Iron sulphate ($Fe_2(SO_4)_3$) and potassium sulphate (a-K_2SO_4) were identified in other combustion experiments on coals from the Teruel Mining District. Moreover, hercynite, gehlenite and esseneite were determined in the combustion experiments with the Santa Eulalia coals.

The Teruel coal

The results obtained in the combustion experiment with the coal from the Teruel power station show a maximum ignition loss between 250 and 450°C (Fig. 4), due to the oxidation of the carbonaceous organic matter. The major inorganic phase transformations undergone during the coal combustion in the present study are shown in Tables 2, 3 and Fig. 4, and may be summarized as follows:

SANTA EULALIA COAL

STA. EULALIA COAL WITH LIME ADDITION

FIG. 6. Evolution of the different inorganic phases during the combustion experiments of the Santa Eulalia coal and Santa Eulalia coal with limestone addition. C, calcite; P, pyrite; G, gypsum; B, bassanite; A, anhydrite; I, illite; K, kaolinite; K-F, K-feldespars; AN, Anorthite; GE, gehlenite; E, esseneite; HE, hercynite; M, mullite; L, lime; H, hematite; Ma, magnetite; Q, quartz. The absolute values for each phase are the intensity in counts per second (proportional to its concentration) of the maximum intensity peak of each phase in the X-ray diffraction pattern of the combustion wastes at different temperatures.

(a) Between 80 and 250°C the dehydration of gypsum to anhydrite through bassanite takes place. Above this temperature the only stable calcium sulphate is anhydrite.

(b) Iron sulphides (pyrite and marcasite) are oxidised during the coal combustion. This oxidation can be directly to iron oxide or through an intermediate iron sulphate stage and than to iron oxide (hematite), depending possibly on the free sulphur and oxygen contents during the combustion. The sulphide decomposition occurs between 350 and 450°C, the iron sulphate

appears above 350°C and its decomposition to sulphur oxides and iron oxides takes place between 600 and 750°C.

Hematite is shown to be stable up to 1400°C, at which temperature the transformation to the reduced oxide (magnetite) takes place. During this transformation the incorporation of aluminium, silicon, calcium and other elements into the magnetite structure occurs, giving rise to complex iron spinels (Fernández-Turiel et al., 1990).The sulphur oxides from the iron sulphide and organic matter oxidations react with the free calcium oxide

giving rise to anhydrite (basis of the ash sulphur retention of the lime addition fluidized bed combustion technology). The free calcium oxide arises from calcite decomposition (which takes place between 350 and 650°C), as well as from the liberation of organic-bonded calcium during organic matter oxidation. The calcite decomposition occurs at relatively low temperatures due to the fact that when coal ignition takes place (at 350°C in the Teruel coal), the combustion temperature is increased substantially due to its calorific value.

(c) Clay minerals lose their crystalline structure as temperature increases through a non-reversible process (Smykatz-Kloss, 1974). This transformation takes place at different temperatures depending on the clay mineral type: (i) kaolinite between 450 and 650°C, at (ii) illite between 800 and 950°C. These amorphous aluminosilicates (silicon spinels) react with the calcium oxide from the calcite decomposition and evolve, with temperature increase (850 and 1100°C), to a calcium aluminosilicate polymorph of anorthite (termed pre-anorthite in this work). The transformation of the calcium aluminosilicate into anorthite takes place between 950 and 1100°C. The alumina and silicon excesses with respect to the calcium oxide give rise to mullite crystallisation above 950°C. Over 1100°C the decomposition of most of the anorthite to tridymite and silicon spinels takes place, they react with the alumina from the vitreous matrix giving rise to mullite crystallization, a very common inorganic phase of fly ash and slags. Quartz is partially consumed in the anorthite crystallization. The melting of quartz and its incorporation into the aluminosilicates of the vitreous matrix begins above 1200°C. The same trend is followed by the free calcium oxide from the anorthite decomposition.

(d) During coal combustion anhydrite is decomposed (Chinchón et al., 1991) to calcium and sulphur oxides at 1060°C. Sulphur dioxide is released to the atmosphere, whereas calcium oxide reacts with the amorphous aluminosilicates giving rise to anorthite crystallization.

The Sabrine, As Pontes and Santa Eulalia coals

The results obtained from the mineralogical studies of the experimental combustion wastes from the Sabrina Mine and As Pontes are similar to those obtained from the Teruel Mining District Coal (Fig. 5). Nevertheless, the occurrence of free calcium oxide and tridymite (high-temperature SiO_2) between 1000 and 1100°C in the combustion of the As Pontes coal must be pointed out.

The Santa Eulalia coal follows a similar trend to the other coals up to 1100°C, but after reaching this temperature, the anorthite content increases, the mullite concentration decreases (Fig. 6) and an aluminium–iron spinel (hercynite, $FeAl_2O_4$) crystallizes after hematite and the alumina from the glassy matrix. These transformations take place at 1200°C. At about 1400°C the combustion waste melts and the decomposition of the anorthite takes place giving rise to a glass-rich ash with minor amounts of mullite.

If limestone is added to the coal combustion a surplus of free calcium oxide in the combustion waste is caused, which brings about:

(a) The fixation of high amounts of sulphur in the solid wastes in the form of anhydrite (Fig. 6). It should be pointed out that the suitable combustion temperature for the maximum sulphur retention in the ash as anhydrite is between 600 and 900°C.

(b) The prevention of the mullite and hercynite occurrence and the crystallization of anorthite, gehlenite and esseneite. At high temperatures the gehlenite gives rise to anorthite. The same process is followed by esseneite over 1200°C which is partially decomposed to anorthite and iron oxide; the latter is incorporated in the vitreous matrix. The surplus of calcium in the ashes at 1400°C gives rise to the melting of the amorphous aluminosilicates and to the stability of anorthite (Fig. 3), although this phase recrystallizes from the vitreous matrix during waste cooling. However, this process of recrystallization is not observed in combustion wastes with a lower calcium content due to the initial decomposition of the anorthite in mullite (high stability phase) and calcium oxide and to the absence of aluminosilicate melting. Furthermore, the high diffusion rate, prior to the melting, leads to the reaction of iron oxides with the vitreous matrix giving rise to hercynite or esseneite, depending on the calcium content.

Aluminosilicate phase transformations

The phase transformations of the aluminosilicate fraction constitute the most complex system during coal combustion. These transformations take place in a closed system which is governed by temperature and the concentration of alumina, silica, iron oxide and lime. Due to the high reactivity of the melt aluminosilicates with calcium, the crystallization occurs after heating and cooling. Moreover it must be pointed out that prior to melting, the system is highly heterogeneous due to the variable composition of individual ash particles. Consequently at a given

temperature, locally different stability fields in the Al–Si–Ca–Fe phase equilibrium (Osborn and Manuan, 1960) are reached. When cationic diffusion commences (immediately prior to melting), a gradation of the chemical composition from the centre to the margin of the ash grains occurs. With the melting processes, which occur at lower temperatures as the calcium content increases, there is an increase in the cationic diffusion leading to system homogeneization and equilibrium. The result is the crystallization of neomorphic phases from the equilibrium Al–Si–Ca–Fe during the cooling of the melt phase. If melting is not reached, the mineral phases may
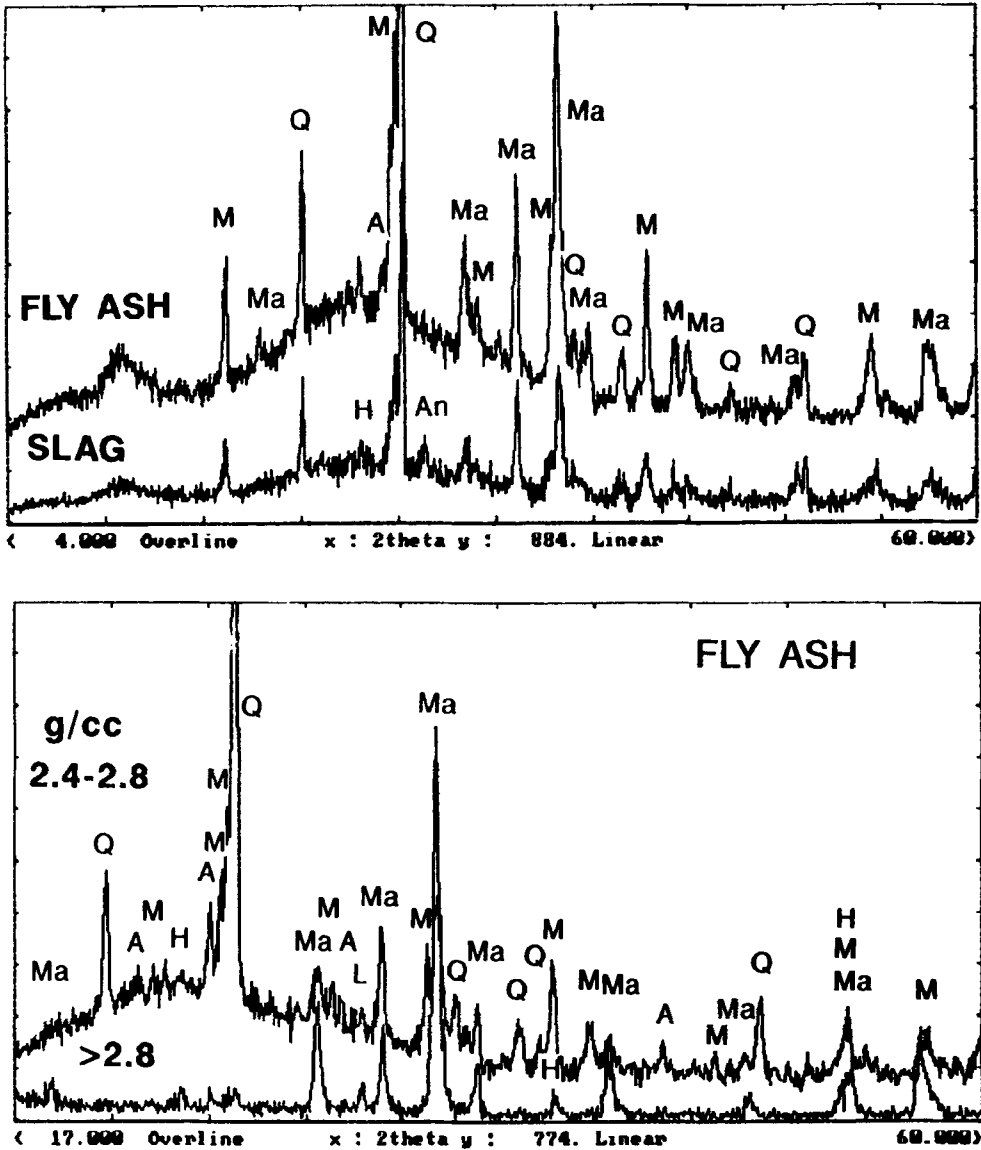

FIG. 7. X-ray diffraction patterns of fly ash and slags from the Teruel power station (whole sample) and of some density fractions of fly ash. Note the detection of lime in the heaviest fraction of fly ash. A, anhydrite; An, anorthite; H, hematite; I, illite; K, kaolinite; L, lime; M, mullite; Ma, magnetite and Q, quartz.

TABLE 4. Mean inorganic phases content (16 samples) of fly ash and slags from the Teruel power station. Results of X-ray diffraction quantification in weight %,

	Fly ash	Slag
Glass*	61.57	73.52
Quartz	6.88	3.97
Mullite	17.58	10.31
Anorthite	<0.3	2.95
Magnetite	12.79	6.94
Hematites	0.45	2.30
Anhydrite	0.70	<0.3

* Quantified by difference.

undergo a variety of solid phase transformations depending on the maximum temperature reached.

In the present study three trends of the aluminosilicate evolution during the coal combustion may be differentiated:
(a) Mineral fraction with low calcium oxide content (Teruel, Sabrina Mine and As Pontes coals). The combustion wastes do not melt at the maximum atemperature reached during the combustion experiments (1400°C). The following sequence of the aluminosilicate transformations during the temperature increase was observed (Figs. 4 and 5):

clays + quartz + lime + hematite →
anorthite + mullite + hematite →
amorphous aluminosilicates + mullite + magnetite

(b) Mineral fraction with intermediate calcium oxide content (Santa Eulalia coal). The combustion wastes melt at 1400°C. The sequence of the aluminosilicate transformations during the temperature increase was (Fig. 6):

clays + quartz + lime + hematite →
    gehlenite + anorthite + hercynite →
        glass + mullite + magnetite

(c) Mineral fraction with high calcium oxide content (Santa Eulalia coal with limestone addition). The combustion wastes melt at 1200°C and during the cooling the vitreous matrix reacts with the lime and the iron oxide giving rise to the crystallization of anorthite and esseneite in smaller proportions. The sequence of the aluminosilicate transformations during the temperature increase was (Fig. 6):

clays + quartz + lime + hematite →
gehlenite + anorthite + esseneite →
glass + anorthite + esseneite.

Mineral content of fly ash and slag

The major inorganic phases in fly ash and slags from the Teruel power station are (Fig. 7): aluminosilicate glass, mullite, quartz, magnetite, anorthite – albite, anhydrite, hematite and lime. Table 4 shows the results of the quantification of the inorganic components in fly ash and slags.

The major differences between the inorganic phases in fly ash and slag from the Teruel power station are (see Table 4 and Fig. 7): (a) the anhydrite is present only in fly ash, and the anorthite only in slags; (b) higher glass content in slags than in fly ash; and (c) higher hematite content and low mullite and magnetite contents in slags than in fly ash.

The presence of anhydrite in fly ash is due to the fact that this phase is formed by the sulphur oxide from the flue gas reacting with the calcium oxide particles after combustion. Thus, the microscopic studies of fly ash have shown the growth of calcium sulphate crystals on the surface of calcium oxide spheres of 10–20 μm diameter. This calcium sulphate is not present in slags due to a lower residence time in the combustion gas and to the lower specific surface of the slags with respect to the fly ash. Furthermore, the slower cooling inside the bigger slag fragments allows anorthite crystallization after the reaction of calcium oxide and the aluminosilicates from the melted vitreous matrix. Moreover, the late slag water cooling in the asher is very fast and gives rise to a higher glass content than in fly ash, and to a higher hematite content due to the oxidizing conditions during the water cooling.

For a more detailed mineralogical study of the fly ash, density separations must be carried out (Furuya *et al.*, 1987). The density yields and the results of the quantitative X-ray diffraction analyses for every density fraction (between 1 and 2.8 g/cc) are shown in Table 5. The results show that:
(a) Except for important fractions of the magnetite and quartz contents, all the crystalline phases are included in a vitreous matrix. This occurrence is microscopically demonstrated, and is clearly shown by the constant glass content distribution through the 1 to 2.8 g/cc fractions, as well as by the presence of quartz (2.65 g/cc), magnetite (5.14 g/cc), hematite (5.20 g/cc), and mullite (3.00 g/cc) in the 1.60 to 2.40 g/cc density fractions. The mullite is included in the vitreous matrix in cenospheres and pleurospheres, and the maximum concentration is found in the 1.00 to 2.00 g/cc density fractions. This fact is supported in the present work by the microscopic studies of fly ash after hydrofluoric treatment (Raask and

TABLE 5. Yield values and inorganic phase contents of the density fractions of fly ash from the Teruel power station. Results of X-ray diffraction quantification in weight %.

Density (g/cc)	Yield	Q	M	A	L	H	M	G*
<1.0	0.4	1.1	29.8	<0.3	<0.3	<0.3	<0.3	69.1
1.0–1.6	1.5	2.3	29.8	<0.3	<0.3	0.3	<0.3	67.7
1.6–2.0	7.5	2.9	28.0	<0.3	<0.3	0.3	0.9	67.9
2.0–2.4	19.4	5.9	21.6	0.4	<0.3	0.4	5.6	66.1
2.4–2.8	56.8	7.0	14.2	0.6	1.3	1.3	7.5	68.1
>2.8	14.4	1.4	3.7	0.8	3.1	3.8	42.9	44.3

*Quantified by difference.

Goetz, 1981) which have shown the occurrence of mullite inside the cenosphere walls with an acicular crystal growth in the glass matrix. Bearing this in mind and the fact that the cenospheres have a very low density, one may find the mullite enriched in the light density fractions of fly ash, as shown by the results.
(b) The calcium oxide is clearly concentrated in the heavy fractions (Fig. 7 and Table 5); however in the whole sample it is not possible to identify it by means of X-ray diffraction (Fig. 7).

Comparison of the mineral content of power plant and laboratory combustion wastes

The major inorganic phases in the fly ash and slags from the Teruel power station are: aluminosilicate glass, mullite, quartz, magnetite, anorthite – albite, anhydrite, hematite and lime. The inorganic phases present in the experimental combustion wastes at 1400°C (combustion temperature similar to those obtained during coal combustion in the Teruel power station boiler) are: aluminosilicate glass, magnetite, mullite and anorthite. The major differences between the inorganic phase composition of both combustion wastes are due to:
(a) The lower residence time of fly ash and slags in the boiler with respect to the experimental ashes. This factor may account for the presence of quartz in fly ash and for the absence of this mineral in the combustion experiment ash. Due to the higher residence time at 1400°C, the quartz reacts with the aluminosilicates to form anorthite and subsequently mullite. The presence of small amounts of free lime in the fly ash may also be due to the lower time of residence in the flame. However in laboratory ash the lime reacts with the aluminosilicates to give rise to the crystallization of anorthite or to the calcium-rich glass.

(b) The influences of the cooling and the gas and particle evacuation controls of the power station. These influences account for the presence of anhydrite in fly ash and for its absence in the combustion experiment wastes. The anhydrite is decomposed in sulphur oxide and lime at 1060°C; this phase must therefore be crystallized in the fly ash after combustion. This fact was microscopically verified due to the location of this sulphate in the external surface of small calcium-rich particles. In the laboratory furnace the combustion gas does not flue with the solid wastes with a progressive cooling, and consequently the fixation of sulphur in the ash as anhydrite does not occur at 1400°C. Moreover, the fast cooling during the water refrigeration of slags in the asher gives rise to the presence of hematite in the slags.

Conclusions

(a) Kaolinite, illite, gypsum, pyrite, marcasite, quartz, microcline and calcite are the major mineral phases present in the coals studied. Furthermore, interlayered clays illite-smectite and iron sulphates with different hydration degrees (szomolnikite, rozenite, melanterite, jarosite, etc.) were identified in coals from the Teruel Mining District.
The results from the microscopical analyses and from the density separations in the Teruel coal show that the clay minerals, quartz and sulphides have a fine grain sized fraction dispersed in the organic matter due to the fact that these mineral phases are present in the light coal fractions, whereas the calcite, feldspars and gypsum are shown to be independent of the organic matrix.
(b) Bassanite, anhydrite, iron sulphate, potassium sulphate, hematite, magnetite, calcium aluminosilicate polymorphic of anorthite,

anorthite–albite, tridymite, mullite, hercynite, gehlenite and esseneite are the inorganic phases produced during coal combustion of the Spanish brown coals studied.

The combustion experiments show that the transformations in the combustion of the coals studied are similar. Two factors control the inorganic phase evolution: namely the sulphur and calcium contents which govern the quantity of anhydrite crystallization (which takes place between 600 and 900°C). Furthermore, high calcium oxide contents cause the fouling of the combustion wastes at relatively low temperatures (1200°C), and prevent the occurrence of mullite and magnetite in the ashes.

(c) The major components in fly ash and slags from the Teruel power station are: aluminosilicate glass, mullite, quartz, magnetite, anorthite–albite, anhydrite, hematite and lime. The major differences between the inorganic constituents in the fly ash and slag from the Teruel power station are: (i) the presence of anhydrite only in fly ash, and anorthite in slags; (ii) a higher glass content in slags; and (iii) a higher hematite content and low mullite and magnetite contents in slags.

The presence of anhydrite in fly ash is due to the fact that this phase is formed after combustion by fixing the sulphur oxide from the flue gas on to the particles of calcium oxide. The slower cooling inside the big slag fragments permits the anorthite crystallization. Moreover, the late slag cooling in the asher is very fast and gives rise to a higher glass content than in fly ash, and to a higher hematite content due to the oxidizing conditions during the water cooling.

(d) A lower residence time of fly ash and slags in the boiler with respect to the experimental ashes can account for the presence of quartz and lime in the fly ash and for the absence of these phases in the experimental wastes. Furthermore, the influence of the cooling and the gas and particulate evaluation controls of the power station accounts for the gas and particulate evacuation controls of the power station accounts for the presence of anhydrite and hematite in the fly ash and slags, respectively. If the influences of these technological factors are borne in mind, it may be possible to predict the inorganic transformations during coal combustion by means of laboratory furnace experiments.

References

Chinchon J. S., Querol, X., Fernández Turiel J. L. and López Soler A. (1991) Environmental impact of mineral transformations undergone during coal combustion. *Environ. Geol. Water Sci.*, **18**, 11–15.

Chung, F. H. (1974a) Quantitative interpretation of X-ray diffraction patterns of mixtures. I: Matrix flushing method for quantitative multicomponent analysis. *J. Appl. Crystallogr.* **7**, 519–25.

Chung, F. H. (1974b) Quantitative interpretation of X-ray diffraction patterns of mixtures. II: Adiabatic principle of X-ray diffraction analysis of mixtures. *J. Appl. Crystallogr.*, **7**, 526–31.

Chung, F. H. (1975) Quantitative interpretation of X-ray diffraction patterns mixtures. III: Simultaneous determination of a set of reference intensities. *J. Appl. Crystallogr.*, **8**, 17–19.

Fernandez Turiel, J. L., Querol, X., Ramirez, C., López Soler, A. and Neikov, C. (1990) Mineralogical characterization of fly ashes from Spanish thermal power stations. *Proc. 15th General Meeting Inst. Mineral. Assoc.*, Beijing, **1**, 170.

Felgueroso, J., Martínez Alonso, A., Martínez Tarazona, M. R., and Tascón, J. M. D. (1988) The determination of mineral matter content of low rank coals. *J. Coal Quality*, **7**, 127–31.

Finkelman, R. B. (1982) Modes of occurrence of trace elements and minerals in coal: an analytical approach. In *Atomic and nuclear Methods in Fossil Energy Research* (R. H. Filby, B. S. Carpenter and R. C. Ragaini, eds.), Plenum, 141–9.

Furuya, K., Miyajima, Y. Chiba, T., and Kikuchi, T. (1987) Elemental Characterization of Particle Size-Density separated Coal Fly Ash by Spectrophotometry. Inductively Coupled Plasma Emission Spectrometry, and Scanning Electron Microscopy-Energy Dispersive X-ray Analysis. *Environ. Sci. Technol.*, **21**, 898–903.

Martínez Alonso, A., Martínez Tarazona, M. R., Cardín, J. M., and Tascón, J. M. D. (1987) The nature and characteristics of mineral matter present in Spanish brown coals used for combustion. *Proc. 1st. Europ. Conf., Influence of inorganic constituents on coal combustion.* **1/6**, 1–8.

Martínez Tarazona, M. R., Palacios, J. M., and Tascón, J. M. D. (1990) SEM–EDX characterization of inorganic constituents of brown coal. *Inst. Phys. Conf. Ser.*, **98**, 327–30.

Martínez Tarazona, M. R., Palacios, J. M., J. M., Martínez Alonso, A. and Tascón, J. M. D. (1990) The characterzation of organomineral components of low-rank coals. *Fuel Proc. Technology*, **25**, 81–87.

Osborn, E. F. and Muan, A. (1960) *Phase equilibrium diagrams of oxide systems.* American Ceramic Society, Columbus, 1025 pp.

Querol, X., Chinchón, J. S., and López Soler, A. (1989) Iron sulfide precipitation sequence in Albian coals from the Maestrazgo Basin (NE Spain). *Int. J. Coal Geol.*, **11**, 171–89.

Querol, X. (1990) *Distribution of sulfur and mineral matter in the Escucha Fm. Coals. Relationship with the geological, sedimentological and diagenetic factors.* (Spanish). Unpubl. Ph.D. Thesis, University of Barcelona, 545 pp.

Querol, X., Fernández Turiel, J. L., Chinchón, J. S., and López Soler, A. (1990) Paragenetic sequence during deposition and diagenesis in lower Cretaceous coal seams of NE Spain. *Proc. 15th General Meeting Int. Mineral Assoc., Beijing*, **2**, 728–30.

Querol, X., Fernández, J. L. López, A., Hagemann, H. W., Dehmer, J., Juan, R., and Ruiz, C. (1991) Distribution of sulfur in coals of the Teruel Mining District (NE Spain). *Int. J. Coal Geol.*, **18**, 327–48.

Querol, X., Alastuey, A., Chinchón, J. S., Fernández, J. L. López, A. (1993) Determination of pyritic sulfur and organic matter in coals by X-ray powder diffraction. *Int. J. Coal Geol.*, **22**, 279–293.

Raask E. (1985) *Mineral Impurities in Coal Combustion. Behaviour, Problems and Remedial Measures.* Springer-Verlag, Berlin, 484 pp.

Raask, E. and Goetz L. (1981) Characterization of captured ash, chimney stack solids and trace elements. *J. Inst. Energy*, **54**, 163–9.

Smith, I. (1987) *Trace elements from coal combustions: emissions.* IEA Coal Research, London, 87 pp.

Smykatz-Kloss W. (1974) *Differential Thermal Analysis. Application and Results in Mineralogy.* Minerals and Rocks, **11**, Springer–Verlag. 185 pp.